Digest Journal of Nanomaterials and Biostructures Vol. 15, No. 4, October-December 2020, p.1075-1088

RESEARCH ON THE MECHANICAL AND TRIBOLOGICAL BEHAVIOR OF SOFT-SOFT CONTACT INTERFACE OF ARTICULAR CARTILAGE

T. ZHANG[a], K. CHEN[b,*], M. WU[b], L. XU[b], D. ZHANG[b]
[a]*School of Mechatronic Engineering, China University of Mining and Technology, Xuzhou 221116, China*
[b]*School of materials and Physics, China University of Mining and Technology, Xuzhou 221116, China*

AC stands the reciprocating friction generated by sports in life. Based on the "soft-soft" contact form of AC in human body, AC specimens acquired from the fresh and healthy bovine knees are selected as the research object in this experiment to study the mechanical and tribological characteristics of AC/AC contact pair. The results show that the creep value of AC is much greater with the increase of the load. The friction coefficient of AC/AC contact pair is significantly lower than that of CoCrMo alloy/AC. The friction coefficient increases with the increase of the load.

(Received August 24, 2020; Accepted October 22, 2020)

Keywords: AC/AC, Creep, Dynamic mechanics, Friction and lubrication, Phospholipid bilayer

1. Introduction

The joint is the biological friction pair with the largest load-carrying capacity in the human body, the surface of which is covered by AC. AC is subject to the reciprocating friction caused by sports in life, whose role is to bear the physiological load of the articular surface and maintain the excellent friction characteristics of the joints. The AC can maintain the excellent friction properties of the joints for a long time with the lubrication of the synovial fluid when the joints move. Meanwhile, AC can effectively absorb energy, relieve the contact stress produced by impact, and protect the subchondral bones from damaging [1-3].AC has an effect in human joints for a long time, during which it is constantly worn and degenerated. However, due to the poor repair ability of cartilage itself, these friction-induced damage on cartilage surface will continue to deteriorate, which affect the overall health of cartilage. Eventually, the damage evolves into serious diseases such as osteoarthritis (OA) [4-5].

AC is a complex soft tissue with elastic structure, which is both strong and flexible and plays a functional and structural role in joints. AC is a biphasic structural material. The liquid phase is mainly composed of water and electrolytes which fills the gap between solid substrates. The solid phase consists of chondrocytes and an extracellular matrix constituted with proteoglycans, collagenous fibers, and non-collagenous proteins without blood vessels, lymphatics, and the nervous system. Chondrocytes form the cellular components that produce and maintain the extracellular matrix. Proteoglycan accounts for about 10-15% of cartilage structure and water

* Corresponding author: cumtck@cumt.edu.cn

absorbing capability, which can increase overall compressive strength. Proteoglycans are mainly protein molecules, which mainly concentrated in the middle layer and less in the deep layer. AC consists of collagen network filled with proteoglycans, which provides hydraulic resistance to mechanical forces and controls water movement within the structure [6].These proteoglycans are hydrated, which cause water to account for a large proportion of the weight and volume of AC. The highest water content is found on the cartilage surface, which can provide incompressible properties. The interaction between these substances may further explain some special properties of AC, such as antifriction and lubrication.

The mechanical and friction lubrication characteristic of AC have been studied systematically by scholars at home and abroad. Federica et al. [7] compared the mechanical properties of healthy cartilage with that of OA cartilage by using a combined experimental–numerical approach. Experimental assessments consist of step wise confined and unconfined compression and tension tests and stress relaxation tests. The numerical model was based on the biphasic theory and mainly included the tension–compression non-linearity. Compared OA samples with normal samples, the static compressive modulus decreased by 55–68%, the permeability increased by 60–80%, the dynamic compressive modulus decreased by 59–64% and the static tension modulus decreased by 72–83%. Jacob et al. [8] has found that a surface layer of hyaluronic acid (HA) complexed with phospholipid bilayer can provide boundary lubrication with the characteristic of high-pressure/low-friction behavior via the hydration lubrication mechanism, which in turn suggests that HA, lubricin, and phospholipid bilayer may act together at the articular surface to provide the remarkable boundary lubrication of the joints. Gao et al. [9] carried out an experimental study on the creep-ratcheting and creep-recovery ratcheting behaviors of AC under creep-fatigue loads. The effect of pre-creep on ratcheting behavior of cartilage was investigated firstly and it is found that the initial ratcheting strain of cartilage presents the larger value due to its pre-creep deformation in spite of the short pre-creep time applied. The ratcheting strain rate decreases with the increase of the increasing pre-creep time the ratcheting strain of sample. These findings showed that the accumulated deformations, including creep deformation and ratcheting deformation, can accelerate the damage of AC. Pawlak et al. [10] found that the frictional behavior of the solid bilayer lubricant is dominated by lamellar slippage of bilayers. The phospholipids content in synovial fluid during inflammation is significantly higher than the normal concentration of phospholipids and a boundary-lubricating ability is poor after the deactivation. Deactivated phospholipid molecule is unable to form bilayers. Gadomski et al. [11] has carried out some work that the cartilage surface was characterized using a combination of the pH, wettability, the interfacial energy and friction coefficient to support lamellar-repulsive mechanism of hydration lubrication. The friction coefficient of bovine joints measured was found to be greatly affected by the pH of the buffer solution. The change in friction was consistently related to the change of charge density of amphoteric surface. Graindorge et al. [12] conducted AC/AC friction tests on fresh and healthy cartilage with and without the surface amorphous layer under both dynamic and static operating conditions. Removal of the surface amorphous layer was not found to change the friction coefficient. However, subsequent staining of specimens indicated that the surface amorphous layer had replenished during the test following loading. Stojanović et al.[13] assessed the role of biological fretting corrosion on the CoCrMo/AC contact interface during sliding process. Experimental results show metal particles still release during sliding contact of CoCrMo alloy/AC despite the extraordinary low friction coefficient measured. Jonathan et al.[14]

performed a series of cyclic unconfined compression tests on AC motivated by in vivo loading conditions and designed to generate mechanical fatigue. A specimen's effective stiffness and resulting thickness significantly are affected with the increase of the number of loading cycles. They attribute permanent loss of mechanical function under cyclic loading to rearrangement and disruption of the collagen network. Boettcher et al.[2] studied the transient dehydration of AC and found that the inability of cartilage to repair itself might be largely compensated by its high endurance and robustness. We therefore speculate that the high resilience of the tissue might minimize the risk of irreversible material failure, reduce the need for repair, and compensate for its poor regenerative abilities to some extent. Chan et al.[15]has found that the boundary lubricant layer in AC was replenish rapidly, which the rate of formation exceed the rate of depletion of the boundary lubricant layer to effectively protect the tissue from mechanical wear.

At present, scholars from home and abroad have conducted many researches on the mechanics and bio-tribology of "hard-soft" contact pair, but few researches on the friction and lubrication mechanism of "soft-soft" contact pair are carried out. Therefore, we mainly study the influence of different loading modes on the creep properties of AC/AC contact pair under the normal load and that of temperature, frequency, shear strain on the dynamic rheology of AC. The effect of the different normal loads and sliding speed on bio-tribological performance of the AC/AC contact pair are also explored, so that the friction lubrication mechanism of AC is revealed and the relationship between the structure and performance of AC is obtained.

2. Materials and methods

2.1. Experimental materials

In the experiment, fresh bovine cartilage on the market is chosen as the upper and lower samples and hollow drills with diameters of 25mm and 6mm are used to drilldown on the cartilage surface, respectively. The lower part of the drilled cartilage samples is trimmed and become smooth, then soaks in normal saline for preservation. Figure 1 shows the plate and pin of the drilled AC, and the CoCrMo alloy is the contrast sample. Ultrapure water was selected as the lubricating medium. Table 1 shows the chemical composition of CoCrMo, and Table 2 shows the related physical mechanical properties.

Fig. 1. Specimens of the AC.

Table 1. Chemical composition of CoCrMo (wt.%)[16].

Element	Co	Cr	Mo	Ni	Fe	Mn	Si	C	N
Mass percent (%)	63.25	28.10	5.90	0.88	0.65	0.63	0.22	0.25	0.12

Table 2. Physical mechanical properties of CoCrMo[16].

Material	Tensile strength, MPa	Yield strength, MPa	Fracture elongation, %	Elastic modulus, GPa	Poisson ratio	Vickers hardness HV
CoCrMo	970	660	18	200	0.3	321

2.2. Experimental methods

In this paper, the mechanical and bio-tribological properties of AC in two contact pairs of AC/AC and CoCrMo alloy/AC under normal loads are mainly investigated. A series of creep controlled trials are carried out on the Rtec friction and wear test machine and the change rules are analyzed. The schematic diagram of the experimental machine is shown in fig.2.Since the stress range of the load-carrying capacity of AC is 0.5-4MPa. In order to explore the change rules of AC, the normal loads are chose in the experiment as follows: 20 N, 30 N, 40 N, and the loading stress is calculated to be within the allowable stress range of AC. Table 3 shows the experimental conditions and parameters of creep of AC.

Meanwhile, a series of sliding friction experiments are carried out on Rtec friction and wear testing machine, the time-varying curves of the friction coefficient are obtained after data processing and biological friction properties in sliding behavior of the contact pair are analyzed. The influence of the normal load and sliding speed on the friction coefficient of the two different friction pairs including CoCrMo alloy/AC and AC/ AC is explored. The experimental parameters of sliding are shown in Table 4.

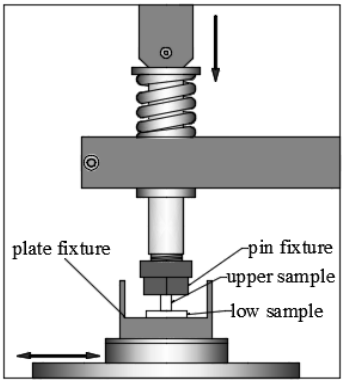

Fig. 2. The schematic diagram of Rtec friction and wear testing machine.

Table 3. Creep experimental parameters of AC.

Experimental conditions and parameters	Scheme 1	Scheme 2	Scheme 3	Scheme 4
Contact pair	AC/AC	CoCrMo / AC	AC / AC	CoCrMo / AC
Lubricating medium	ultrapure water	ultrapure water	ultrapure water	ultrapure water
Loading mode	single loading	single loading	Continuous loading	Continuous loading
Normal load /N	20、30、40	20、30、40	10，20，30，40	10，20，30，40
Testing time/h	1	1	4	4

Table 4. Sliding friction experimental parameters.

Experimental conditions and parameters	Scheme 1	Scheme 2	Scheme 3
Contact pair	CoCrMo/ AC	AC/AC	AC/ AC
Lubricating medium	ultrapure water	ultrapure wate r	ultrapure water
Normal loading/N	20	20、30、40	20
Sliding rate/(mm/s)	2	2	2、5、10、15、20
Testing time/h	1	1	1
Frequency/Hz	1	1	1

3. Results

3.1. Creep of AC/AC contact under single loading mode

Fig. 3 shows the creep curves of two contact pairs under different loading conditions. The curves show that the creep of AC increases gradually with time, the initial growth rate is fast and then slows down, and the creep value of AC increases with the increase of load. When normal loads are 20N, 30N and 40N, the creep deformations are 0.623 mm, 0.927 mm and 1.162 mm, respectively. The creep value increases from 0.623mm to 1.162mm, an increase of 0.539mm. When normal loads are 20N, 30N and 40N, the creep values of CoCrMo alloy/AC contact pair are 0.425 mm, 0.465 mm and 0.585 mm, respectively. When the normal load increases from 20 N to 40 N, the creep value increases from 0.425 mm to 0.585 mm, an increase of 0.160mm.Obviously, the creep value of AC increases as the load increases.

The creep values of two contact pairs including AC/ AC and CoCrMo alloy/ AC under normal load of 20 N are 0.623mm and 0.425mm, respectively. The creep values under 30 N normal load are 0.927mm and 0.465mm, respectively. The creep values under 40 N normal load are 1.162 mm and 0.585 mm, respectively. Under different normal loads, the creep values of the two contact pairs are significantly different, and the creep value of the AC / AC contact pair are twice that of the CoCrMo alloy/ AC contact pair. The creep curve of AC/AC contact pair has a larger slope than that of CoCrMo alloy/AC contact pair, which means that the creep of AC/AC contact pair has a higher growth rate than that of CoCrMo alloy/ AC contact pair.

The creep behavior is realized by the movement of water and macromolecules inside the AC and creep deformation occurs when liquid is extruded from the tissue during loading. Rapid deformation occurs at the beginning and liquid exude rapidly. As the content of the remaining

liquid decreases, the flow rate gradually becomes slower, and so the transudation ratio becomes slower until the equilibrium is reached and the fluid stops flowing. As natural AC is a solid-liquid coupling material, whose elastic modulus is much lower than that of CoCrMo alloy. That is to say, compared with AC, CoCrMo alloy has a greater hardness. Both upper and lower specimens of AC/AC contact pair will deform, so the creep of contact pair composed of AC will be significantly different, and even the creep value of “soft-soft” contact pair is twice that of "hard-soft" contact pair.

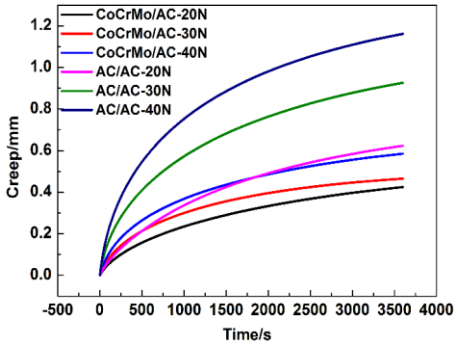

Fig. 3. Creep curves of two contact pairs under different loads.

3.2. Creep of AC/AC contact under continuous loading mode

Fig. 4 shows the creep curves of two contact pairs under continuous loading. The phenomenon of instantaneous elastic creep of AC/AC at the beginning of the experiment conforms to hooke's law. The creep values of AC/AC are 0.95037, 1.30952 and 1.54172 respectively and that of CoCrMo alloy/AC are 0.32147, 0.5314 and 0.68492 respectively after loading at 10N, 20N and 30N for 1h. The results are obvious: the creep value of AC/AC is much greater than that of CoCrMo alloy/AC, mainly because the hardness of CoCrMo alloy is much greater than that of AC, and the AC is more prone to deformation than CoCrMo alloy under the same conditions.

For continuous creep of AC, water and macromolecules are extruded rapidly in contact area of AC at initial loading and the creep value has spiked, but cartilage contained the high viscosity fluids that is not permitted to squeeze the space of two contact surfaces out ,which result in the accumulation of pressure, so that AC can support relatively large load. But if continuous loading is applied and large load is maintained for a long time, lubricants will run out, AC begins to get thin, the structure gets hard, and the creep value will decrease.

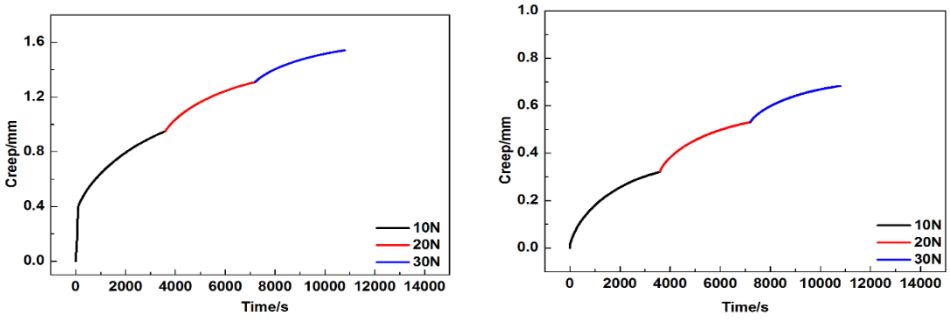

a) *b)*

Fig. 4. Curves of continuous creep of different contact pairs a) AC/ AC b) CoCrMo/AC.

3.3. Dynamic rheology of AC

Fig. 5 shows the change curves of storage modulus, loss modulus and loss factor of AC with shear strain. Elastic deformation and viscous deformation will occur when the material

deforms. The storage modulus represents the energy stored by the elastic deformation and reflects the elastic property of the material. The loss modulus represents the energy consumed by the viscous deformation and reflects the viscous property of the material. As can be seen from the figure, the storage modulus decreases with the increase of shear strain, the loss modulus has been in a steady state, and the corresponding loss factor has been rising. When the shear strain is less than 0.84% which is in the stage of low deformation, the storage modulus keeps decreasing but is still higher than the loss modulus. The loss modulus increases slowly, but remains relatively low on the whole. The initial stage of low shear strain, that is, before the shear strain is below 0.171%, the storage modulus is much larger than the loss modulus, and the loss factor is always at a low value. The storage modulus of AC decreases continuously with the increase of the shear strain, while the loss modulus gradually increases. When shear strain is greater than 0.84%, which is in the stage of high deformation, storage modulus has been gradually decreases, the loss modulus show a trend of increasing first and then decreasing with the increase of shear strain and has been greater than the storage modulus.

At the beginning of low strain, the natural AC generates almost pure elastic deformation. At the late stage of low shear strain, the proportion of viscous deformation gradually increases, but AC is still dominated by elastic deformation. In the stage of high shear strain, the ratio of viscous deformation is larger than that of elastic deformation, but the deformation is dominated by viscous deformation. The loss factor of AC has been steadily increasing with the increase of strain, which is mainly due to the increase of internal collagen network deformation, internal friction increases and then viscous flow gradually increases with the increasing of strain.

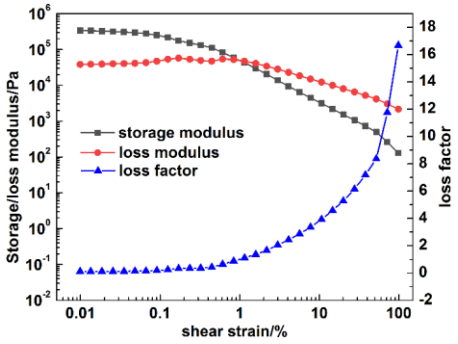

Fig. 5. Curves of storage modulus, loss modulus and loss factor of AC with shear strain.

Fig. 6 shows the changing curves of storage modulus, loss modulus and loss factor of AC in the temperature range of 25℃-40℃.The curves show that with the increasing of temperature, the storage modulus and loss modulus decrease gradually and the loss factor increases gradually. The loss factor is the ratio of the loss modulus to the storage modulus. Therefore, the loss factor tends to increase with the increasing of temperature. When the temperature rises from 25℃ to 28℃, the rate of increasing of loss factor is large which increase by 6.92% from 0.592 to 0.633.When the temperature rises from 28℃ to 40℃, the rate of increasing of loss factor increases slowly, which only increase by 3.48% from 0.633 to 0.655. That is to say, when the temperature is low, the change of temperature has a greater impact on the loss factor, but the high temperature has a smaller impact on the loss factor.

In general, the loss factor rises from 0.592 at 25℃ to 0.655 at 40℃, which increases by 10.64%. The temperature has a great influence on the loss factor. In the temperature range (25℃ -40℃) of measurement, the storage modulus is always much higher than the loss modulus. Therefore, the deformation of AC in this temperature range has always been dominated by elastic deformation, which can show good dynamic mechanical properties.

High temperature causes the loss of liquid phase in cartilage and the internal structure of cartilage is also damaged, which lead to the decrease of elastic modulus and viscous modulus. However, the storage modulus itself is much larger than the loss modulus, and the magnitudes decreased is also greatly different. Compared with the storage modulus, the decrease of loss modulus is almost negligible.

The temperature change has a greater effect on the loss factor at low temperature stage, while at the high temperature stage, the temperature has a smaller effect on the loss factor. Guess is that the higher the temperature is, the more serious the loss of liquid phase and the damage of internal structure inside of the cartilage are and the decreasing of storage modulus is much faster than that loss modulus, which may also be related to the normal temperature of cattle. The lower the temperature is below the normal range, the greater the influence of the temperature change on the mechanical behavior of AC is.

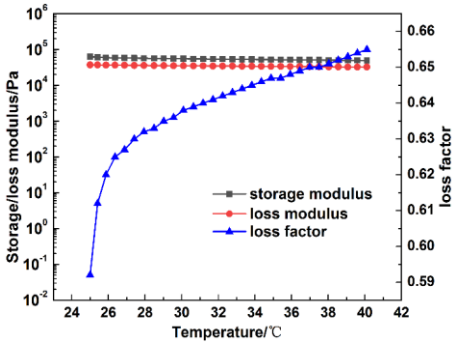

Fig. 6. Curves of storage modulus, loss modulus and loss factor of AC with temperature.

Fig. 7 shows the changing curves of storage modulus, loss modulus and loss factor of AC with frequency. It can be seen from the figure that the storage modulus keeps a steady state with the increasing of frequency. The loss modulus keeps basically stable with the increasing of frequency and has a slow increasing trend. The changes of storage modulus and loss modulus make the loss factor keep a steady increasing in the frequency range measured. However, the storage modulus is always larger than the loss modulus with the increase of frequency, that is to say, the loss factor is always less than 1.

The natural AC is viscoelastic in the whole frequency range and has a good stored energy structure. When the AC is impacted, more energy is stored. The deformation of AC in this frequency range is always dominated by elastic deformation, which can offset the impact and protect the joints. Consequently, AC can show better dynamic mechanical properties.

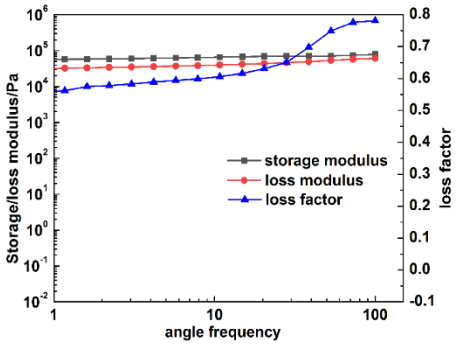

Fig. 7. Curves of storage modulus, loss modulus and loss factor of AC with shear angle frequency.

3.4. Bio-tribologcy of AC/AC contact

Fig. 8 shows the time-varying curves of sliding friction coefficient of AC/AC contact pair and CoCrMo alloy/AC contact pair when the sliding speed is 2 mm/s and the normal load is 20 N. The figure shows that the trend of the time-varying curves of friction coefficient of different contact pair is roughly same. In the initial stage, due to the sliding behavior is not stable, initial friction coefficient will increase rapidly and the friction process tends to stabilize with time, which is determined by hydraulic bearing characteristics of cartilage. The hydraulic bearing mechanism of AC begins to react in the initial stage and the viscoelasticity of cartilage makes this response have a process. The hydraulic bearing process in gaps of AC gradually stabilize with time and the superficial layer of cartilage have an even load capacity, thus the friction coefficient tends to level off.

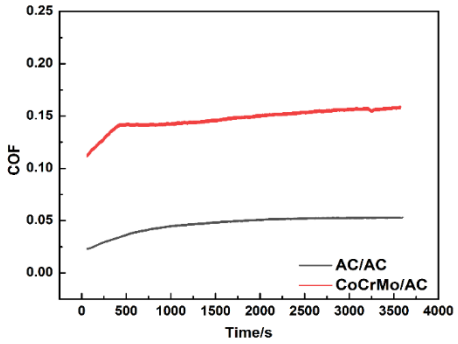

Fig. 8. Time-varying sliding friction coefficient curves of different contact pair.

Fig. 9 shows the time-varying curves of sliding friction coefficient of AC/AC contact pair when the sliding velocity is 2 mm/s and the normal loads are 20N, 30N and 40N, respectively. As can be seen from the figure, when the normal loads are 20 N, 30 N and 40 N, the final stable friction coefficients are 0.0375, 0.0490 and 0.0610, respectively. The friction coefficient gradually increases with the increase of the normal load. When the load increases from 20 N to 30 N, the friction coefficient increases by 30.67%.When the load increases from 30 N to 40 N, the friction coefficient increases by 24.49%. The reason why high load has little effect on friction coefficient is that the increase of load will improve its lubrication condition under a certain load.

On the one hand, AC which has a strong viscoelasticity is prone to elastic deformation, easy to produce better geometric consistency with the contact surface, and conducive to the formation of thicker liquid film to achieve micro-elastic fluid lubrication; On the other hand, AC which has a strong permeability makes synovial fluid infiltrate or extrudes under a certain load. The extruded fluid can play a lubricating role to reduce friction and wear and play a buffer role to achieve elasto-hydrodynamic lubrication.

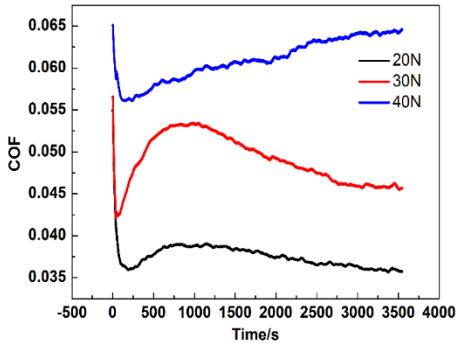

Fig. 9. Time-varying sliding friction coefficient curves of AC/AC contact pair under different normal loads.

Fig. 10 shows the time-varying curves of sliding friction coefficient of AC /AC under normal load of 20 N and sliding speed of 2 mm/s, 5 mm/s, 10 mm/s, 15 mm/s and 20 mm/s ,respectively. Fig. 11 shows the histogram of the average friction coefficient of AC/AC contact pair at different sliding speeds. As can be seen from the figure, the final stable friction coefficients are 0.0375, 0.0316, 0.0170, 0.0356 and 0.0285 at the sliding speed of 2 mm/s, 5 mm/s, 10 mm/s, 15 mm/s and 20 mm/s, respectively. That is to say, the friction coefficient first decrease, then increase and decrease again with the increase of the sliding speed. When the sliding speed is 2 mm/s, the friction coefficient is the maximum, while when the sliding speed is 10 mm/s, the friction coefficient is the minimum. The variation trend of friction coefficient under different sliding speed is basically the same, which is first increased and then tend to stabilize. This is because the surface of AC is not completely smooth and need to carry on the unceasing wearing in the initial stage of friction process, so as to the friction coefficient gradually increases. As the friction continues, the process tends to be stable and the friction coefficient becomes gradually smooth.

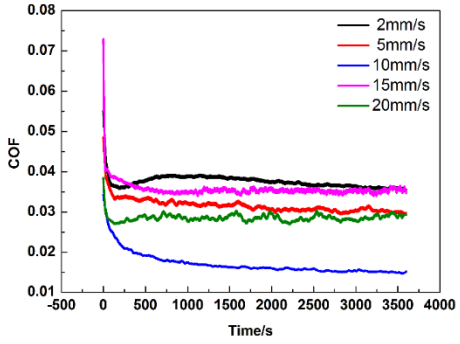

Fig. 10. Time-varying sliding friction coefficient curves of AC/AC contact pair under different sliding speeds.

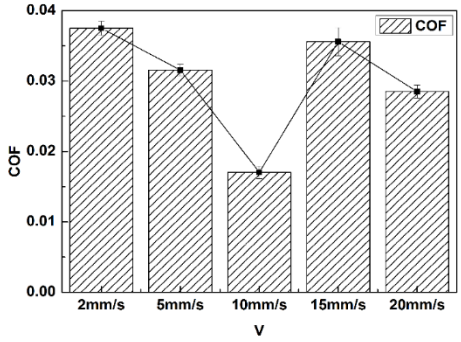

Fig. 11. Bar chart of average friction coefficient of AC/AC contact pair under different sliding speeds.

4. Discussions

AC is a highly structured biological material and the mechanical response is associated with time and load, which shows biphasic characteristics that the interaction between solid phase and liquid phase [17,18]. The mixed lubrication or boundary lubrication exists not only in the low speed but also at higher load. Solid-liquid biphasic characteristics of AC play an important role in reducing friction and strengthening the lubricating performance.

The friction force of AC contact pair is mainly determined by the load on the solid phase. The surface amorphous layer can significantly change the load distribution between the solid phase and liquid phase in the friction process of AC/AC contact pair, so that the dynamic balance relationship of mutual transformation exists between the load carried by the solid phase and that carried by the liquid phase of AC. The deformation of AC increases with the increase of the load, which cause more fluid to flow out of the cartilage and the load is transferred from the solid phase to the liquid phase. Consequently, the load carried by liquid phase decrease and the load carried by solid phase increase. This shows that the deformation amount of AC is positively correlated with the load carried by solid phase and the friction coefficient of contact pair of AC is also directly correlated with the deformation amount. That is to say, the friction coefficient tends to be stable with the extension of loading time. Meanwhile, the larger the normal load is, the greater the friction coefficient is. On the other hand, the deformation of AC is within the frequency range of elastic deformation. With the increase of deformation amount, the deformation of internal collagen network increases and internal friction increase and then viscous flow increases gradually. At the same time, the temperature of the contact interface also increases, which cause the internal structure of the cartilage to be damaged, including porous structure of cartilage itself. Above all, the viscoelasticity decreases and the friction coefficient increases.

Petelska [19] think that the friction coefficient is highly reliant on the electrostatic interaction between the two cartilage surfaces. The low friction coefficient of the two sliding cartilage sides that have the same charge is associated with the electrostatic repulsion of a charged AC/AC pair. The electrostatic repulsion between the two cartilage surfaces is conducive to the formation of a thicker water layer between the cartilage surfaces, so that the lubrication mode changes from boundary lubrication to mixed lubrication or even hydrodynamic lubrication, which significantly reduces the friction between the two cartilage surfaces. Gadomski[20] suggests that

the interaction between phospholipids and composites of hyaluronic acid fibers leads to the formation of inverted cylindrical micelles around the fibers, which absorb the mass force exerting on the articular cartilage. Hydrophilic heads of repeated arrangement also have a buffer effect. Reverse micelles can decrease the friction coefficient by changing frictional form and promote lubrication in the joints.

The phospholipid in the surface amorphous layer of AC has a chemical inertness and hydrophilic-hydrophobic structure, which enables the phospholipid to form a lamellar structure. The pressure distribution between the AC surface is non-uniform and the friction coefficient measured in boundary lubrication mode is independent of speed or that measured in the mixed lubrication decreases with the increase of speed [21].

As shown in Fig. 12, the lamellar slippage of the bilayer lipid membranes occur in the surface amorphous layer and macromolecules of synovial fluid act like roller-bearings between two cartilage surfaces, which make sliding change into rolling to reduce the friction coefficient[22]. As the extension of loading time, the surface amorphous layer covering the AC under a certain sliding speed is worn and even removed and the friction coefficient tends to rise. The surface amorphous layer exists regeneration mechanism, which can realize the surface layer replenishment during the test following loading. When friction coefficient is higher, the layer structure is formed by the phospholipid bilayer via the lamellar-repulsion mechanism, which can promote AC sliding. After that, the AC surfaces quickly translate into stable low friction. Therefore, the different lubrication mechanism of cartilage surface and the self-replenishment of surface amorphous layer can realize that the friction coefficient increases first, then decreases and increase again under different sliding speed.

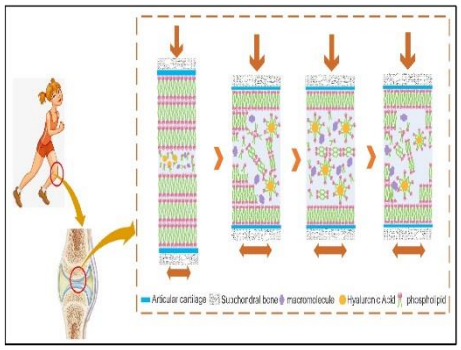

Fig. 12. Schematic diagram of cartilage contact surfaces during friction.

5. Conclusions

Though the study of the mechanical and bio-tribological characteristics of AC/AC contact pair and CoCrMo alloy/AC contact pair, we find that the creep curves all rise rapidly and then gradually slow down under different load and contact pair conditions. The creep rate is much faster with the increase of the load, which cause the elastic deformation of low strain to be transformed into the viscous deformation of high strain, and even the creep value of "soft-soft" contact pair is twice than that of "hard-soft" contact pair. The viscoelasticity decreases which the increase of the temperature in the frequency range. The friction coefficient of AC/AC contact pair is significantly

lower than that of CoCrMo alloy/AC contact pair. The friction coefficient of AC/AC contact pair decreases first, then increases and decreases again with the increase of sliding speed.

Acknowledgments

This research is supported by National Natural Science Foundation of China (Grant No. 51705517, 51875564), Natural Science Foundation of Jiangsu Province (Grant No. BK20160257), China Postdoctoral Science Found (Grant No. 2018M630622).

References

[1] S. Treppo, H. Koepp, E. C. Quan, A. A. Cole, K. E. Kuettner, A. J. Grodzinsky, Journal of Orthopaedic Research **18**(5), (739) 2000.
[2] K. Boettcher, S. Kienle, J. Nachtsheim et al., Acta Biomaterialia **29**(1), (180) 2015.
[3] D. W. Lee, X. Banquy, J. N. Israelachvili, Proceedings of the National Academy of Sciences **110**(7), (567) 2013.
[4] Z. Dai, J. Gong, Journal of Biomedical Engineering **23**(3), (669)2006.
[5] E. D. Bonnevie, D. Galesso, C. Secchieri, L. J. Bonassar, Journal of Orthopaedic Research **36**(5), (1456) 2018.
[6] A. Abazari, N. M. Jomha, J. A. W. Elliott, L. E. McGann, Cryobiology **66**(3), (201) 2013.
[7] F. Boschetti, G. M. Peretti, Biorheology **45**(3), (337) 2008.
[8] S. Jahn, J. Seror, J. Klein, Annual Review of Biomedical Engineering **18**(1), (235) 2016.
[9] L. Gao, D. Liu, H. Gao, L. Lv, C. Zhang, Materials Science and Engineering C **94**, (988) 2019.
[10] Z. Pawlak, A. Mrela, M. Kaczmarek, M. Cieszko, Biosystems **177**, (44) 2019.
[11] Z. Pawlak, A. Gadomski, M. Sojka, W. Urbaniak, P. Beldowski, Colloids and Surfaces B: Biointerfaces **146**, (452) 2016.
[12] S. Graindorge, W. Ferrandez, E. Ingham, Z. Ingham, Z. Jin, P. Twigg, J. Fisher, Proceedings of the Institution of Mechanical Engineers, Part H: Journal of Engineering in Medicine **220**(5), (597) 2006.
[13] B. Stojanović, C. Bauer, C. Stotter, T. Klestil, S. Nehrer, F. Frank, M. R. Ripoll, Acta biomaterialia **94**, (597) 2019.
[14] J. T. Kaplan, C. P. Neu, H. Drissi, N. C. Emery, D. M. Pierce, Journal of the mechanical behavior of biomedical materials **65**, (734) 2017.
[15] S. M. T. Chan, C. P. Neu, G. DuRaine, K. Komvopoulos, A. H. Reddi, Journal of biomechanics **45**(14), (2426) 2012.
[16] H. Xu, K. Chen, D. Zhang, X. Yang, Journal of Biomater Science-Polymer Edition **29**(311), (1) 2018.
[17] H. Zhou, Biotribological mechanism of articular cartilage, Shanghai Jiao Tong University, (70) 2013.
[18] H. Fujie, K. Imade, Biosurface and Biotribology **1**(2), (124) 2015.
[19] A. D. Petelska, K. Kazimierska-Drobny, K. Janicka, T. Majewski, Coatings **9**(4), (264) 2019.

[20] A. Gadomski, Z. Pawlak, A. Oloyede, Tribology Letters **30**(2), (83) 2008.
[21] J. Charnley, Annals of the Rheumatic Diseases **19**(1), (10) 1960.
[22] C. H. Yu, Jay. T. Groves, Medical & Biological Engineering & Computing **48**(10), (955) 2010.